Int. J. Electrochem. Sci., 15 **(2020)** 5166 – 5178, doi: 10.20964/2020.06.30

International Journal of
ELECTROCHEMICAL
SCIENCE
www.electrochemsci.org

Degradation of 2,4-Dichlorobenzoic Acid by Coupled Electrocatalytic Reduction and Anodic Oxidation

Ning Li, Xiaozhe Song, Hui Wang[*]

College of Environmental Science and Engineering, Beijing Forestry University, Beijing 100083, PR China
[*]E-mail: wanghui@bjfu.edu.cn

Received: 4 January 2020 / *Accepted:* 12 March 2020 / *Published:* 10 May 2020

Dual effects of cathodic dechlorination and oxidative decomposition of 2,4-dichlorobenzoic acid (2,4-DCBA) can be achieved using electrochemical reduction-oxidation technology. The removal efficiency was improved by optimizing the experimental conditions affecting electrode activity and contaminant degradation. The 2,4-DCBA removal efficiency reached 90.8% at a current density at 50 $mA \cdot cm^{-2}$, initial pH of 5, and sodium sulfate concentration of 0.05 $mol \cdot L^{-1}$, with a 2,4-DCBA concentration of 20 $mg \cdot L^{-1}$. Furthermore, a good total organic carbon removal efficiency of 81.6% was achieved in the electrocatalytic reduction and oxidation process, with the present system retaining high stability after many experiment cycles. The reaction mechanism under different conditions is discussed, which provides new approaches to the degradation of chlorinated organic compounds.

Keywords: 2,4-dichlorobenzoic acid, electrochemical reduction-oxidation, optimal conditions, dechlorination, oxidation reaction

1. INTRODUCTION

Chlorinated organic compounds, which can persist in water for long periods and have harmful effects, have received increasing attention [1, 2]. As chlorinated organic compounds contain chlorine atoms, they are typical refractory toxic and harmful organic pollutants [3-5]. To eliminate chlorinated organic compounds from water, electrocatalytic reduction technology has attracted interest owing to its high dichlorination efficiency and fewer toxic intermediates [6]. During electrocatalytic hydrodechlorination (EHDC), the entire carbon skeleton is usually retained, with C-Cl bonds selectively broken under metal catalysis. Active hydrogen (H^*) from the reduction of water and the decomposition of H_2 can displace chlorine atoms from pollutants [7, 8]. However, most treatment processes for 2,4-dichlorobenzoic acid (2,4-DCBA) have focused on hydrodechlorination [9-11], while the further degradation of dechlorination products still needs to be studied. The oxygen reduction reaction (ORR)

in the cathodic compartment comprises a two-electron reduction process to form hydrogen peroxide (H_2O_2), which is a green oxidizer that further transforms into oxidative radicals for pollutant mineralization [12]. Combined reduction-oxidation has been reported to degrade chlorinated organic compounds [13]. The electron reduces H^+ to generate H^* species as the indirect pathway for dechlorination [3,4], while the intermediate products are transformed into small molecule acids or H_2O and CO_2 by oxidation processes [7].

The relative kinetics of EHDC and the hydrogen evolution reaction (HER) of 2,4-dichlorophenol on a Pd nanoparticle catalyst have been regulated by controlling the solution pH to optimize the EHDC reaction [14]. The ORR performance of a Pd-Fe/graphene cathodic catalyst for H_2O_2 production was improved when filled with oxygen under alkaline conditions [7]. Therefore, the target reaction can be developed and reaction efficiency improved by adjusting the experimental parameters.

In this study, the influence of different conditions on removal efficiency was investigated by single factor analysis using a catalytic cathode containing cobalt single-atom catalysts. 2,4-DCBA was selected as the target pollutant to evaluate cathodic dechlorination and oxygen reduction performance. The impact of current density and initial pH on the removal efficiency was evaluated, and appropriate electrolyte and initial pollutant concentrations were determined to improve 2,4-DCBA degradation. Furthermore, the degradation mechanism of 2,4-DCBA at different reaction stages was explained by detecting the concentration changes of Cl^- and total organic carbon (TOC). The stability of the system was also evaluated with respect to practicality.

2. EXPERIMENTAL

2.1 Electrolysis experiments

The Co-loaded sulfide graphene (Co-SG) catalyst was synthesized by thermal reduction [15, 16]. Through characterization of the catalyst morphology and structure, the catalyst with a cobalt content of 1% was uniformly distributed on graphene in the form of single atom, and showed good performance in hydrodechlorination and oxygen reduction. Using Co-SG to prepare the catalytic cathode was consistent with the reported method [17].

The divided electrochemical reactor was based on anodic oxidation and cathodic reduction processes. The apparatus consisted of anodic and cathodic compartments divided by a polyester fabric diaphragm, and a gas compartment to achieve combined reduction-oxidation process requirements, as shown in Fig. 1. The anode and cathode were Ti/IrO_2/RuO_2 and Co-SG electrodes (40 mm × 60 mm), respectively. The initial pH value was controlled using sulfuric acid and sodium hydroxide. The electrolytes were sodium sulfate solutions of different concentrations. 2,4-DCBA solutions of different concentrations were prepared for comparison. The segmented sparging method was used during experiments in the cathodic compartment, with H_2 introduced for the first 60 min, and air introduced for the next 60 min. Cl^- removed from the cathodic compartment was transferred to the anodic compartment through the diaphragm and then oxidized to chlorine gas to leave the system during the EHDC process. After 60 min, the ORR process proceeded with air injection to produce oxidizing substances for pollutant

degradation. Simultaneously, the constant oxidation reaction in the anodic compartment also helped to remove pollutants.

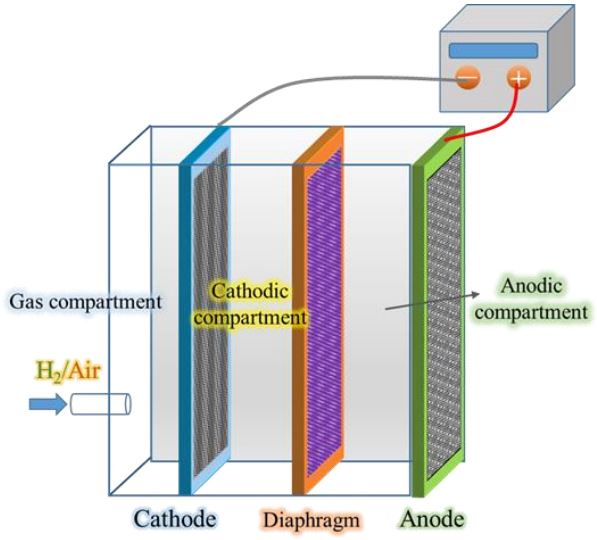

Figure 1. Diagram of electrocatalytic reduction-oxidation reaction device.

The 2,4-DCBA treatment processes conformed to first-order kinetics [17, 18]:

$$\ln\frac{[C]_0}{[C]_t}=k\cdot t$$

where $[C]_0$ is the initial 2,4-DCBA concentration ($mg\cdot L^{-1}$), $[C]_t$ is the 2,4-DCBA concentration at a time of t min, and k is the apparent removal rate constant.

2.2 Analysis

The concentrations of 2,4-DCBA and benzoic acid (BA) were determined by high-performance liquid chromatography (HPLC-2030, Japan), using a mobile phase composed of methanol and 0.2% H_3PO_4 solution (6:4, v/v). The H_2O_2 concentration was determined from the change in the absorbance of a potassium iodide solution after reacting with H_2O_2 using a spectrophotometer (U-2910, Hitachi). The Cl^- concentration was analyzed by ion chromatography (IC-3000 Dionex, USA), using water and NaOH solution (250 $mmol\cdot L^{-1}$) as the mobile phase. TOC was measured using a TOC analyzer (TOC4000, Shimadzu).

3. RESULTS AND DISCUSSION

3.1 Process optimization for 2, 4-DCBA degradation

3.1.1 Effect of current density

As shown in Fig. 2(a), the 2,4-DCBA removal efficiency in the cathodic compartment was significantly increased at a current density 50 $mA\cdot cm^{-2}$ compared with that at 30 $mA\cdot cm^{-2}$. The

degradation reaction of 2,4-DCBA fitted a pseudo first-order reaction (R^2> 0.95) from a semi-logarithmic figure of the 2,4-DCBA concentration change over time at different current densities. When the current density was 50 mA·cm^{-2}, the maximum kinetic constant for the cathodic compartment was 0.0137 min^{-1}, as shown in Table 1. Enhanced performance was attributed to the augmented reactive species content in the cathodic compartment during different processes with higher current densities [19]. The reduction of H^+ and production of H^* were limited in the cathodic compartment during the EHDC process, resulting in low reactivity at 30 mA·cm^{-2} [20]. However, both the removal efficiency and k value decreased at a current density of 60 mA·cm^{-2}, which resulted in the HER proceeding and the synthesized substance being thermally decomposed in the oxidation process. The H_2 bubbles released on the cathode surface might negatively affect the adsorption of 2,4-DCBA at a current density over 50 mA·cm^{-2}, resulting in a reduced removal efficiency [21].

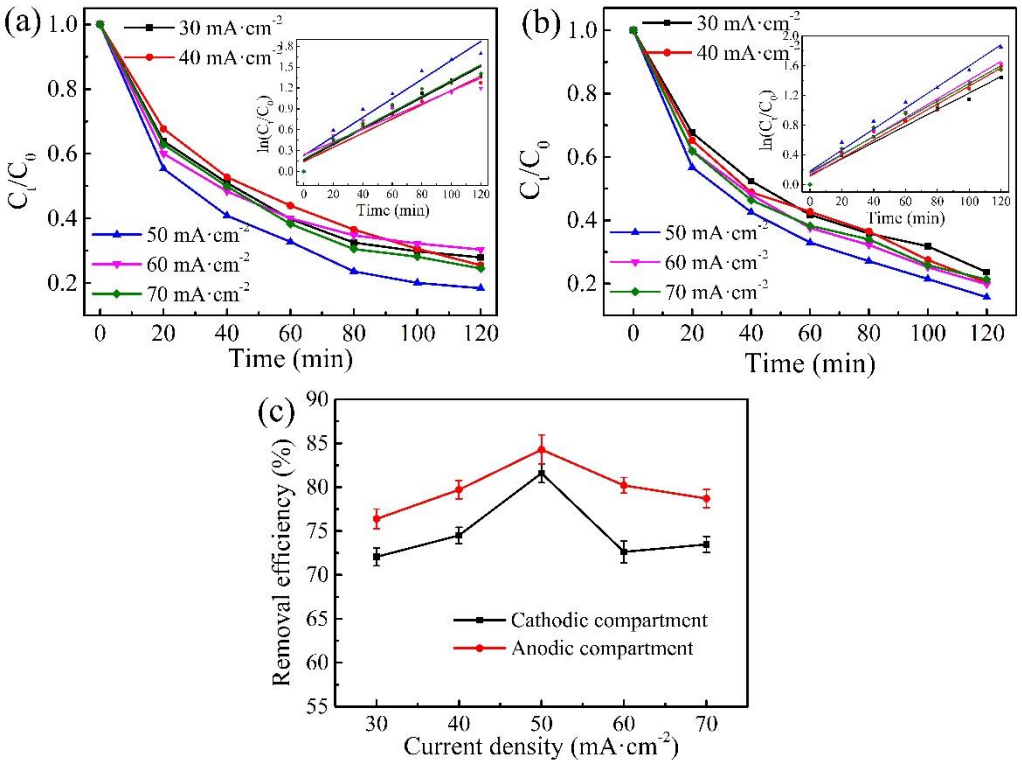

Figure 2. Effect of 2,4-DCBA concentration over time with different current densities in (a) cathodic and (b) anodic compartments. Conditions: Initial pH, 5; electrolyte, 0.1 mol·L^{-1} Na_2SO_4; initial 2,4-DCBA concentration, 40 mg·L^{-1}. Kinetic equations are inserted. (c) Influence of current density on the removal efficiency of 2,4-DCBA after 120 min.

As shown in Fig. 2(b), increasing the current density improved removal efficiency in the anodic compartment. At a current density of 50 mA·cm^{-2}, the k value was 0.0142 min^{-1}, which was greater than that at 30 mA·cm^{-2} (0.0111 min^{-1}), as shown in Table 1. This indicated that the increase in current density promoted the reaction rate. The improved removal efficiency at 50 mA·cm^{-2} might contribute to the increasing content of hydroxyl radicals (•OH) produced as current density increased [22]. Inevitably,

exposing the anode to high-current operation resulted in accelerated passivation long-term. Accordingly, the side reactions were intensified and active species generation was inhibited [23]. As shown in Fig. 2(c), 2,4-DCBA reached highest removal efficiencies of 81.6% and 84.3% in the cathodic and anodic compartments, respectively, at 50 $mA \cdot cm^{-2}$. Therefore, 50 $mA \cdot cm^{-2}$ was selected to ensure the electrical potential was sufficient for the reaction.

Table 1. Effect of current density on pseudo-first-order kinetic rate parameters.

Current density ($mA \cdot cm^{-2}$)	$k(min^{-1})$		R^2	
	Cathodic compartment	Anodic compartment	Cathodic compartment	Anodic compartment
30	0.0104	0.0111	0.9592	0.9727
40	0.0108	0.0121	0.9769	0.9766
50	0.0137	0.0142	0.9896	0.9719
60	0.0092	0.0126	0.9836	0.9764
70	0.0113	0.0120	0.9747	0.9641

3.1.2 Effect of initial pH

As the initial solution pH in the cathodic compartment increased, less 2,4-DCBA was removed. This indicated that the removal efficiency under acidic conditions was higher than that under alkaline conditions, as shown in Fig. 3(a). At pH 5, the rate constant of the cathodic compartment reached a maximum value of 0.0131 min^{-1} (Table 2). H^+ in water was reduced at the cathode surface to form a large amount of H^* to attack the C-Cl bonds on the benzene ring of 2,4-DCBA, resulting in a rapid decrease in the 2,4-DCBA concentration (Eqs. 1 and 2). At an initial pH of 3, the EHDC efficiency was reduced owing to excessive acidity. H^* adsorbed on the catalyst surface readily aggregates to generate H_2 (Eq. 3), resulting in less H^* utilization [14, 24].

$$H^+ + Co + e^- \rightarrow [H^*]Co + OH^- \quad (1)$$

$$[H^*]Co + RCl \rightarrow Co + RH + H^+ + Cl^- \quad (2)$$

$$2[H^*] \rightarrow H_2\uparrow \quad (3)$$

The removal efficiency of the anodic compartment is more efficient under acidic conditions [17]. Oxidative free radicals can directly attack 2,4-DCBA aided by electrons, resulting in a better removal efficiency at 86.7% at an initial pH of 5, as shown in Figs. 3(b) and 3(c). As the reaction progressed, the pH in the cathodic compartment was close to 13, while that in the anodic compartment was close to 1 when the initial pH was 5, as shown in Fig. 3(d). The removal efficiency in the cathodic compartment was still increasing. This depended chemisorbed H_2 on the catalyst surface, which decomposed to form H^* continuously with H_2 flow into the gas compartment and direct electron reduction on the cathode surface. The 2,4-DCBA removal efficiency increased to around 60% during EHDC. The reduction of oxygen to H_2O_2 under alkaline conditions at a later stage also contributed to further pollutant conversion [25]. The removal efficiency of 2,4-DCBA in the cathodic compartment finally reached 83.3%.

Therefore, 2,4-DCBA showed a relatively high removal efficiency both in the cathodic and anodic compartments at an initial pH of 5.

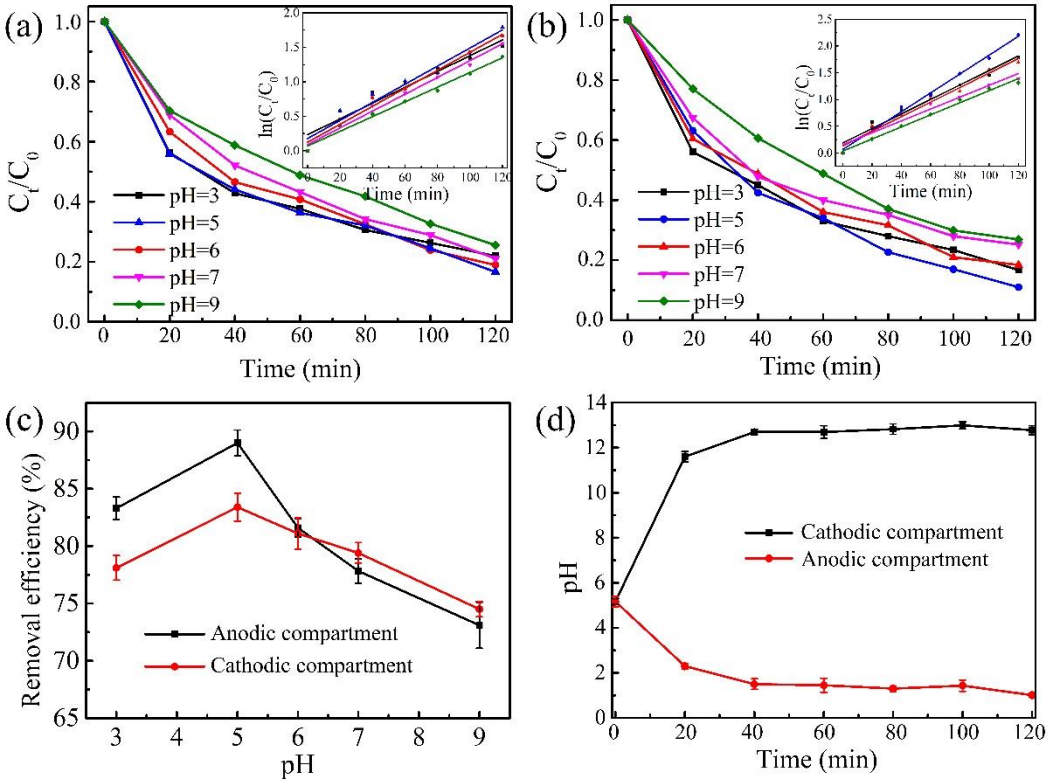

Figure 3. Effect of 2,4-DCBA concentration over time with different initial pH values in (a) cathodic and (b) anodic compartments. Conditions: current density, 50 $mA \cdot cm^{-2}$; electrolyte, 0.1 $mol \cdot L^{-1}$ Na_2SO_4; initial 2,4-DCBA concentration, 40 $mg \cdot L^{-1}$. Kinetic equations are inserted. (c) Influence of initial pH on removal efficiency of 2,4-DCBA after 120 min; (d) change in pH value over time.

Table 2. Effect of initial pH on pseudo-first-order kinetic rate parameters.

Initial pH	k(min^{-1})		R^2	
	Cathodic compartment	Anodic compartment	Cathodic compartment	Anodic compartment
3	0.0136	0.0115	0.9648	0.9727
5	0.0176	0.0131	0.9944	0.9581
6	0.0136	0.013	0.9768	0.9807
7	0.0111	0.0122	0.9551	0.9881
9	0.0113	0.0107	0.9915	0.9890

3.1.3 Effect of electrolyte concentration

Electrolyte concentration affects the electrochemical reaction rate by changing the current and voltage [31]. The Na_2SO_4 electrolyte is stable because it does not produce new oxidizing substances to affect the experimental process [26]. The trend in 2,4-DCBA removal efficiency at different electrolyte concentrations from 0.01 to 0.15 mol·L^{-1} was explored at a current density of 50 mA·cm^{-2} and initial pH of 5.

In the Na_2SO_4 concentration range of 0.01-0.05 mol·L^{-1}, the removal efficiency of 2,4-DCBA increased with increasing electrolyte concentration, with a positive correlation between electrolyte concentration and removal efficiency, as shown in Figs. 4(a) and 4(b). The k value of the cathodic compartment increased from 0.0129 to 0.0160 min^{-1} in the Na_2SO_4 concentration range of 0.01-0.05 mol·L^{-1}, as shown in Table 3. At a Na_2SO_4 concentration of 0.05 mol·L^{-1}, the 2,4-DCBA removal efficiency in the cathodic compartment reached a maximum value of 88.7% (Fig. 4(c)). This indicated that increasing the Na_2SO_4 concentration accelerated ion collisions in the reaction system and enhanced mass transfer in the EHDC [27].

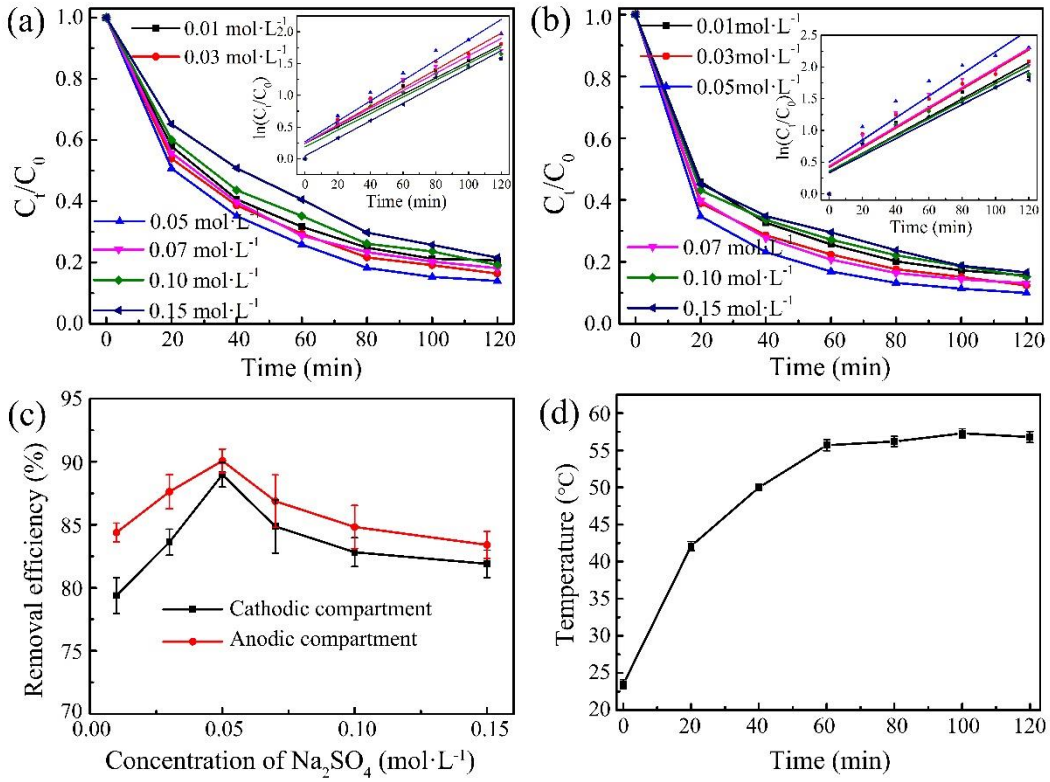

Figure 4. Effect of 2,4-DCBA concentration over time with different electrolyte concentrations in (a) cathodic and (b) anodic compartments. Conditions: Current density, 50 mA·cm^{-2}; initial pH, 5; initial 2,4-DCBA concentration, 40 mg·L^{-1}. Kinetic equations are inserted. (c) Influence of Na_2SO_4 concentration on 2,4-DCBA removal efficiency after 120 min; (d) curve of temperature against time with a Na_2SO_4 concentration of 0.05 mol·L^{-1}.

When the reaction entered the oxidation stage saturated with air, the reaction solution temperature increased to around 55°C, and •OH generation was accelerated, improving the removal efficiency, as shown in Fig. 4(d) [17]. Furthermore, the removal efficiency and k value showed a slow downward trend when the Na_2SO_4 concentration exceeded 0.05 mol·L^{-1}. When the concentration in the cathodic compartment was over 0.05 mol·L^{-1}, the Na^+ concentration in the cathodic compartment also increased, which shielded the active sites under the action of the electric field. Furthermore, the thermal energy generated was smaller and the reaction rate slower at the same current because solution resistance was reduced, resulting in reduced pollutant removal efficiency [28].

The solution conductivity improved with increasing Na_2SO_4 concentration, which facilitated the generation of •OH and promoted the oxidization of 2,4-DCBA in the anodic compartment. The 2,4-DCBA removal efficiency in the anodic compartment reached a maximum value of 89.9%, as shown in Fig. 4(b). However, the high electrolyte concentration caused electrolyte ions to be adsorbed on the electrode surface, hindering the migration of 2,4-DCBA to the electrode surface, and reducing the oxidation of 2,4-DCBA at the anode [29]. Some side reactions occurred, which affected the progress of the main reaction. In conclusion, 0.05 mol·L^{-1} was determined to be most suitable for further degradation from Fig. 4(c).

Table 3. Effect of Na_2SO_4 concentration on pseudo-first-order kinetic rate parameters.

Na_2SO_4 (mol·L^{-1})	k(min^{-1})		R^2	
	Cathodic compartment	Anodic compartment	Cathodic compartment	Anodic compartment
0.01	0.0129	0.0143	0.9822	0.9878
0.03	0.0144	0.0154	0.9721	0.9888
0.05	0.0160	0.0174	0.9694	0.9867
0.07	0.0137	0.0155	0.9792	0.9684
0.10	0.0131	0.0138	0.9583	0.9899
0.15	0.0138	0.0134	0.9826	0.9854

3.1.4 Effect of initial 2,4-DCBA concentration

The 2,4-DCBA initial concentration was also a key factor in the electrocatalytic reduction and oxidation process because it affects the diffusion control of 2,4-DCBA. To explore whether the cathode catalyst showed good removal efficiency at different initial concentrations, a series of 2,4-DCBA concentration gradients (10-50 mg·L^{-1}) were configured for detection.

As shown in Figs. 5(a) and 5(b), the removal efficiency decreased as the initial 2,4-DCBA concentration increased. As shown in Table 4, the k values and removal efficiency showed no obvious differences at low concentrations between 10 and 20 mg·L^{-1}. Introducing 2,4-DCBA at 20 mg·L^{-1} resulted in removal efficiencies in the cathodic and anodic compartments after 120 mins of 90.8% and 92.4%, respectively (Fig. 5(c)). When the initial concentration was low, the electrochemical reaction rate was higher than the diffusion rate, such that 2,4-DCBA was effectively removed [28]. When the initial 2,4-DCBA concentration added was increased to 50 mg·L^{-1}, the removal efficiencies in the cathodic and

anodic compartments were reduced to 81.0% and 84.8%, respectively (Fig. 5(c)). The same conclusions can be drawn from the reaction kinetic parameters shown in Table 4. The rate constant at 10 mg·L^{-1} was 0.0189 min^{-1}, which was better than that at 50 mg·L^{-1} (0.0124 min^{-1}; Table 4). At a fixed current density, the increase in initial concentration slightly reduced the 2,4-DCBA degradation rate both in the cathodic and anodic compartments.

The absolute 2,4-DCBA removal concentration appeared to increase, even when the removal efficiency decreased with increasing initial concentration, as shown in Fig. 5(d). When the initial concentration was increased from 10 to 50 mg·L^{-1}, the absolute removal concentration was increased from 9.1 to 39.4 mg·L^{-1}. These data also showed that the catalytic cathode still had a high removal capacity for 2,4-DCBA at high concentration. At high concentrations during the degradation stage, active species can react with pollutants faster and less side reactions occur in the cathodic compartment. This reduces the capacity loss during the reaction and increases the absolute removal of 2,4-DCBA [30-32]. This same conclusion for the anodic compartment might be due to the high concentration of pollutants moved to the anode surface for oxidation simultaneously. Therefore, the prepared catalytic cathode showed good removal efficiency for 2,4-DCBA at both high and low concentrations.

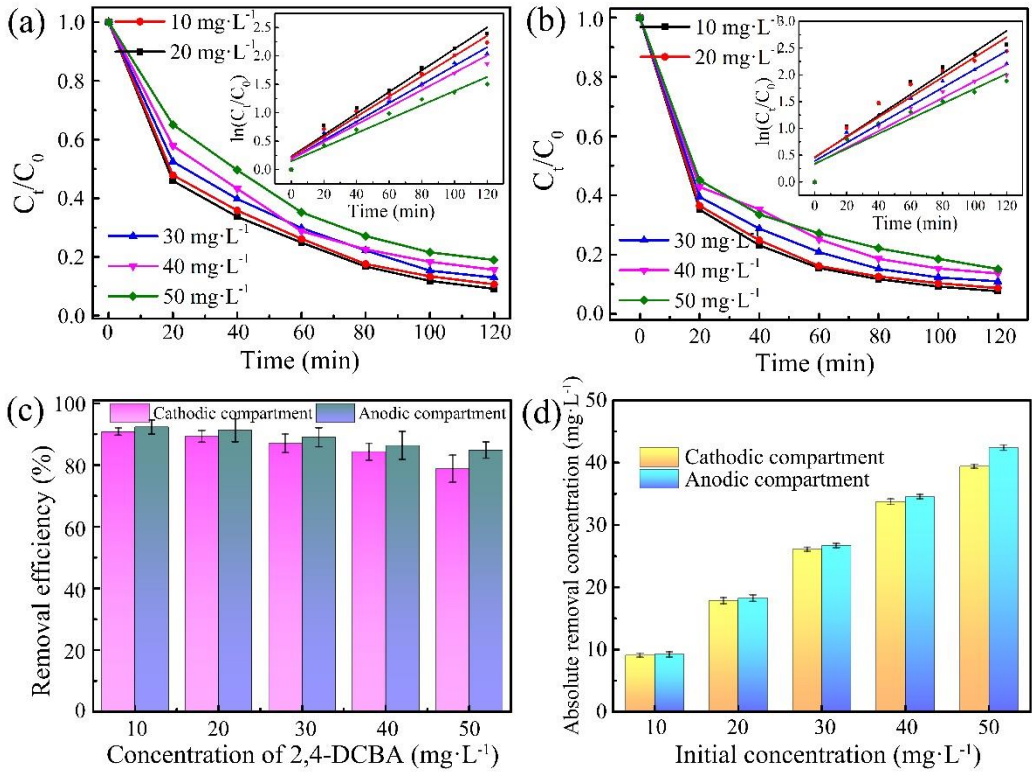

Figure 5. Effect of 2,4-DCBA concentration over time with different 2,4-DCBA concentrations in (a) cathodic and (b) anodic compartments. Conditions: current density, 50 mA·cm^{-2}; initial pH, 5; electrolyte, 0.05 mol·L^{-1} Na_2SO_4. Kinetic equations are inserted. (c) Influence of initial 2,4-DCBA concentration on removal efficiency after 120 min; (d) absolute removal concentration with different initial 2,4-DCBA concentrations.

Table 4. Effect of initial 2,4-DCBA concentrations on pseudo-first-order kinetic rate parameters.

Initial 2,4-DCBA concentration ($mg \cdot L^{-1}$)	$k(min^{-1})$		R^2	
	Cathodic compartment	Anodic compartment	Cathodic compartment	Anodic compartment
10	0.0189	0.0197	0.9741	0.9813
20	0.0183	0.0194	0.9737	0.9849
30	0.0164	0.0171	0.9757	0.9729
40	0.0152	0.0155	0.9653	0.9821
50	0.0124	0.0140	0.9651	0.9983

3.2 Electrocatalytic degradation of 2,4-DCBA

From the above exploration of different conditions, the effective conditions for 2,4-DCBA degradation were optimized. The following experiments were performed under optimal conditions (current density, 50 $mA \cdot cm^{-2}$; initial pH, 5; electrolyte, 0.05 $mol \cdot L^{-1}$ Na_2SO_4; initial 2,4-DCBA concentration, 20 $mg \cdot L^{-1}$). The conversation of 2,4-DCBA to BA, as shown in Fig. 6(a), resulted in a rapid decrease in 2,4-DCBA concentration in the first 30 min, which might be due to the porous structure of the catalyst adsorbing the pollutant on the cathode surface and accelerating the EHDC process. As the reaction time increased, the 2,4-DCBA concentration in the cathodic compartment gradually decreased, while the BA content increased to 81.8%. This result showed that the C-Cl bond of 2,4-DCBA was effectively broken in the EHDC stage, which aided the subsequent oxidation reaction.

As shown in Fig. 6(b), without 2,4-DCBA in the solution, the H_2O_2 concentration in the system increased and then decreased over time. The maximum concentration was 17.31 $mg \cdot L^{-1}$ without 2,4-DCBA after 40 min of air flow. In the presence of 2,4-DCBA, the change trend of H_2O_2 was consistent with absence of 2,4-DCBA. The maximum concentration of H_2O_2 after adding 2,4-DCBA was 10.9 $mg \cdot L^{-1}$, which was smaller than that in the absence of 2,4-DCBA. As H_2O_2 has a certain oxidizing capacity, some of the H_2O_2 produced in the cathodic system can be directly used for the degradation process, which reduces the H_2O_2 concentration [33]. In the electrolytic system, H_2O_2 is mainly derived from the two-electron ORR. The electrolyte in the cathodic compartment gradually became alkaline during the reaction (Fig. 3d). Oxygen was catalytically reduced to produce H_2O_2 on the surface of the Co-SG catalytic cathode. H_2O_2 can decompose to •OH and $\bullet O_2^-$ through catalysis under alkaline conditions (Eqs. 4-6) for further degradation. The H_2O_2 decomposition rate was greater than its generation rate, resulting in the H_2O_2 concentration gradually decreasing [17].

$$O_2+H_2O+2e^- \rightarrow HO_2^-+OH^- \quad (4)$$

$$HO_2^-+H_2O \rightarrow OH^-+H_2O_2 \quad (5)$$

$$HO_2^- + H_2O_2 \rightarrow \cdot OH+\cdot O_2^-+H_2O \quad (6)$$

The chloride ion concentration in the cathodic compartment increased rapidly within 60 min, while the removal efficiency of TOC reached 25.5%, which was significantly lower than that of the anode (61.3%), as shown in Fig. 6(c). This indicated that the hydrodechlorination reaction of 2,4-DCBA

dominated the cathodic compartment and achieved a good Cl^- removal efficiency. This was mainly because Co metal on the cathode catalyst has a strong hydrogen absorption capacity and generates H^* [34]. Before benzene ring cleavage, no obvious change in TOC concentration was observed in the EHDC. As time proceeded, the Cl^- and TOC concentrations in the cathodic compartment gradually decreased. Chloride ions removed by the cathodic compartment entered the anode through the separator owing to the electrostatic effect. The ORR dominated the cathodic compartment when filled with air. As H_2O_2 and other oxidizing free radicals produced by the cathode can oxidatively decompose the benzene ring structure, the TOC removal efficiency began to increase to 61.9% at 80 min.

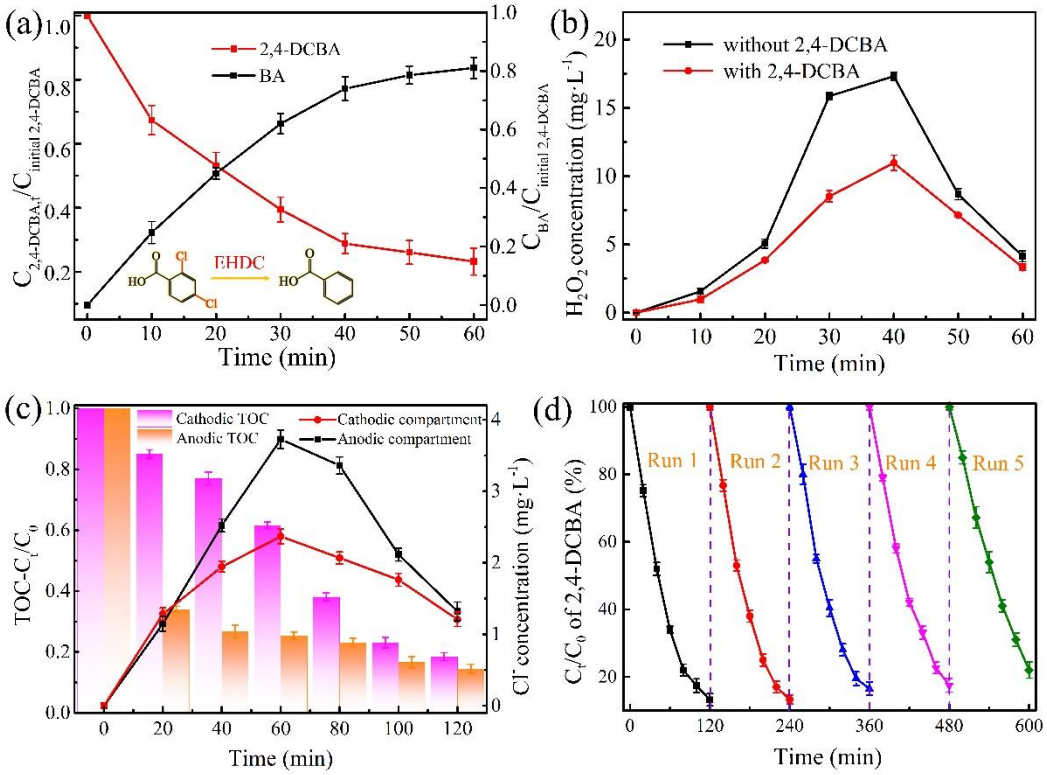

Figure 6. (a) Removal efficiency of 2,4-DCBA and generation of BA; (b) Co-SG-catalyzed cathode production of H_2O_2 concentration over time in electrolyte with and without 2,4-DCBA; (c) Cl^- and TOC concentrations over time during degradation; (d) change in 2,4-DCBA concentration during five cycles.

As the chlorine ions migrated to the anodic compartment and were continuously oxidized, chlorine gas dissociated from the electrolytic system, and the Cl^- concentration tended to rise and then fall [35]. For the anodic compartment, the oxidized free radicals generated directly attacked the benzene ring structure through the continuous oxidation reaction. As a result, the TOC concentration decreased continuously. 2,4-DCBA was finally converted into small-molecule acids or carbon dioxide. The TOC removal efficiency in the anodic compartment reached 85.4%, which was slightly higher than that of the cathodic compartment (81.6%). This might be due to the continuous oxidation reaction resulting in more thorough mineralization of 2,4-DCBA. The effective removal efficiency of Cl^- was calculated to be 83.1%. Through the above analysis, the cathode-based electrochemical reduction-oxidation process achieved Cl^- removal and TOC reduction, indicating that 2,4-DCBA was effectively degraded.

Electrode stability is also a key factor affecting the application of electrocatalysis technology. Therefore, the stability of the Co-SG-catalyzed cathode for 2,4-DCBA degradation was investigated through repeated degradation, as shown in Fig. 6(d). The removal efficiency in the cathodic compartment only decreased by 9.1% after five consecutive repeat degradation experiments, indicating the good repeatability of the Co-SG cathode. The slight decrease in the removal efficiency compared with the first cycle might be due to a decrease in the adsorption effect of the porous structure of the catalyst. The stability increased the practicability of the catalytic electrode.

4. CONCLUSIONS

The removal of 2,4-DCBA under different conditions was explored and a corresponding mechanism was proposed. The catalytic cathode performed dechlorination at pH 5 under H_2, which reduced the toxicity of the pollutants. The current density (50 $mA \cdot cm^{-2}$) and Na_2SO_4 concentration (0.05 $mol \cdot L^{-1}$) positively affected 2,4-DCBA degradation. Furthermore, the removal efficiency reached over 80% within the initial concentration range studied. The results of dechlorination and mineralization were explained by the Cl^- and TOC removal efficiencies of 83.1% and 81.6%, respectively. These results showed that 2,4-DCBA can be degraded with over 90% efficiency under the optimal reaction conditions. This process also provides a reference for the degradation of other chlorinated organic compounds.

ACKNOWLEDGEMENTS
We gratefully acknowledge financial support from the National Natural Science Foundation of China (No. 21872009), and Beijing Forestry University Outstanding Young Talent Cultivation Project (No. 2019JQ03007).

References

1. Y.J. Feng, L.S. Yang, J.F. Liu and B.E. Logan, *Environ. Sci.-Wat. Res. Technol.*, 2 (2016) 800.
2. Z. Cao, X. Liu, J. Xu, J. Zhang, Y. Yang, J.L. Zhou, X.H. Xu and G.V. Lowry, *Environ. Sci. Technol.*, 51 (2017) 11269.
3. Y.L. Han, C.J. Liu, J. Horita and W.L. Yan, *Appl. Catal. B-Environ.*, 188 (2016) 77.
4. Y.F. Wu, L. Gan, S.P. Zhang, H.O. Song, C. Lu, W.T. Li, Z. Wang, B.C. Jiang and A.M. Li, *J. Hazard. Mater.*, 356 (2018) 17.
5. S.K. Song, Y.M. Su, A.S. Adeleye, Y.L. Zhang and X.F. Zhou, *Appl. Catal. B-Environ.*, 201 (2017) 211.
6. D.F. Laine and I.F. Cheng, *Microchem J.*, 85 (2007) 183.
7. X.Z. Song, Q. Shi, H. Wang, S.L. Liu, C. Tai and Z.Y. Bian, *Appl. Catal. B-Environ.*, 203 (2017) 442.
8. C. Lim and S.-I. Pyun, *Electrochim. Acta*, 39 (1994) 363.
9. C. Sun, S.A. Baig, Z.M. Lou, J. Zhu, Z.X. Wang, X. Li, J.H. Wu, Y.F. Zhang and X.H. Xu, *Appl. Catal. B-Environ.*, 158 (2014) 38.
10. Z.M. Lou, Y.Z. Li, J.S. Zhou, K.L. Yang, Y.L. Liu, S.A. Baig and X.H. Xu, *J. Hazard. Mater.*, 362 (2019) 148.
11. Z.M. Lou, J.S. Zhou, M. Sun, J. Xu, K.L. Yang, D. Lv, Y.P. Zhao and X.H. Xu, *Chem. Eng. J.*, 352 (2018) 549.

12. X.Z. Song, N. Li, H. Zhang, H. Wang, L.Y. Wang and Z.Y. Bian, *J. Power Sources*, 435 (2019) 226771.
13. Q. Shi, H. Wang, S.L. Liu, L. Pang and Z.Y. Bian, *Electrochim. Acta*, 178 (2015) 92.
14. G.M. Jiang, K.F. Wang, J.Y. Li, W.Y. Fu, Z.Y. Zhang, G. Johnson, X.S. Lv, Y.X. Zhang, S. Zhang and D. Fan, *Chem. Eng. J.*, 348 (2018) 26.
15. P.Q. Yin, T. Yao, Y.E. Wu, L.R. Zheng, Y. Lin, W. Liu, H.X. Ju, J.F. Zhu, X. Hong, Z.X. Deng, G. Zhou, S.Q. Wei and Y.D. Li, *Angew. Chem.-Int. Edit.*, 55 (2016) 10800.
16. Y. Hou, Z.H. Wen, S.M. Cui, S.Q. Ci, S. Mao and J.H. Chen, *Adv. Funct. Mater.*, 25 (2015) 872.
17. D.D. Xu, L. Zhang, H. Wang and Z.Y. Bian, *Chem. Eng. J.*, 358 (2019) 1371.
18. J.S. Zhou, Z.M. Lou, J. Xu, X.X. Zhou, K.L. Yang, X.Y. Gao, Y.L. Zhang and X.H. Xu, *Chem. Eng. J.*, 358 (2019) 1176.
19. S. Song, J.Q. Fan, Z.Q. He, L.Y. Zhan, Z.W. Liu, J.M. Chen and X.H. Xu, *Electrochim. Acta*, 55 (2010) 3606.
20. Y. Liu, L. Liu, J. Shan and J.D. Zhang, *J. Hazard. Mater.*, 290 (2015) 1.
21. G. Jiang, M. Lan, Z. Zhang, X. Lv, Z.M. Lou, X.H. Xu, F. Dong and S. Zhang, *Environ. Sci. Technol.*, 51 (2017) 7599.
22. C. Wang, J.F. Niu, L.F. Yin, J.X. Huang and L.A. Hou, *Chem. Eng. J.*, 346 (2018) 662.
23. Y. Fan, Z.H. Ai and L.Z. Zhang, *J. Hazard. Mater.*, 176 (2010) 678.
24. B. Liu, H. Zhang, Q. Lu, G.H. Li and F. Zhang, *Sci. Total Environ.*, 635 (2018) 1417.
25. S. Salomé, R. Rego and M.C. Oliveira, *Mater. Chem. Phys.*, 143 (2013) 109.
26. Y.C. Wang, M. Chen, C. Wang, X.Y. Meng, W.Q. Zhang and Z.F. Chen, *Chem. Eng. J.*, 374 (2019) 626.
27. X.Z. Bian, Y. Xia, T.T. Zhan, L. Wang, W. Zhou, Q.Z. Dai and J.M. Chen, *Chemosphere*, 233 (2019) 762.
28. X.J. Wei, H. Wang, Z.Y. Bian and G. Lu, *Adv. Mater. Res.* 356 (2012) 1323.
29. J.M. Chen, Y.J. Xia and Q.Z. Dai, *Electrochim. Acta*, 165 (2015) 277.
30. Y. Samet, L. Agengui and R. Abdelhédi, *J. Electroanal. Chem.*, 650 (2010) 152.
31. Y. Wang, Z.Y. Shen and X.C. Chen, *J. Hazard. Mater.*, 178 (2010) 867.
32. B. Garza-Campos, D. Morales-Acosta, A. Hernández-Ramírez, J. Guzmán-Mar, L. Hinojosa-Reyes, J. Manríquez and E.J. Ruiz-Ruiz, *Electrochim. Acta*, 269 (2018) 232.
33. Z. Guo, Y.B. Xie, J.D. Xiao, Z.J. Zhao, Y.X. Wang, Z.M. Xu, Y. Zhang, L.C. Yin, H.B. Cao and J.L. Gong, *J. Am. Chem. Soc.*, 141 (2019) 12005.
34. S. Baranton and C. Coutanceau, *Appl. Catal. B-Environ.*, 136 (2013) 1.
35. D.D. Xu, X.Z. Song, W.Z. Qi, H. Wang and Z.Y. Bian, *Chem. Eng. J.*, 333 (2018) 477.